2020 *Chem. Mater.* **2010,** *22,* 2020–2026
DOI:10.1021/cm903783w

CHEMISTRY OF MATERIALS
Article

Enhanced Performance of Bulk Heterojunction Solar Cells Using Block Copoly(3-alkylthiophene)s

Guoqiang Ren,[†] Pei-Tzu Wu,[†] and Samson A. Jenekhe*[,†,‡]

[†]*Department of Chemical Engineering and* [‡]*Department of Chemistry University of Washington, Seattle, Washington 98195-1750*

Received October 15, 2009. Revised Manuscript Received January 24, 2010

The photovoltaic properties, charge transport, and morphology of a series of diblock conjugated copolymers, poly(3-butylthiophene)-*b*-poly(3-octylthiophene) (P3BT-*b*-P3OT), were investigated as a function of block composition. Bulk heterojunction solar cells comprising blends of P3BT-*b*-P3OT and [6,6]-phenyl-C_{71}-butyric acid methyl ester ($PC_{71}BM$) were found to have power conversion efficiencies as high as 3.0%, which represents factors of 1.6−9 enhancements compared to those of the homopolymers made under similar conditions. Imaging of P3BT-*b*-P3OT/$PC_{71}BM$ blends by atomic force microscopy and transmission electron microscopy revealed interpenetrating network with 11−18 nm crystalline polymer domains. The zero-field space charge limited current mobility of holes ($\sim(1-3) \times 10^{-4}$ cm^2 V^{-1} s^{-1}) was similarly enhanced in the diblock copolymer solar cells compared to the homopolymers. These results demonstrate that block conjugated copolymers offer a promising approach to advanced materials for polymer solar cells and that the block composition is an attractive means to optimize the materials.

Introduction

Polymer solar cells are of worldwide research interest because of their potential as low-cost and easy-to-fabricate solar energy-to-electric power conversion devices.[1−19] Bulk heterojunction (BHJ) devices,[8,9] in which a donor polymer is blended with a fullerene derivative or other acceptor material, have emerged as the most efficient polymer solar cells to date. Among donor polymers in fullerene-based BHJ solar cells, regioregular poly(3-hexylthiophene) (P3HT) has been the most widely investigated and has resulted in some of the highest power conversion efficiencies (3 - 5% PCE).[1,2,10,11] However, BHJ solar cells similarly made from related regioregular poly(3-alkylthiophene)s (P3ATs), such as poly(3-butylthiophene) (P3BT), poly(3-octylthiophene) (P3OT), and poly(3-decylthiophene) (P3DT), have very poor efficiencies ($< 0.5 - 1\%$ PCE).[12] Although recent efforts, such as nanowire-based BHJ solar cells[18] and extensive materials processing and device optimization,[19] have pushed the power conversion efficiency above 3.0% for P3BT-based BHJ solar cells, the inferior photovoltaic properties of other P3ATs compared to P3HT remain to be fully explored and understood. In addition to the greatly reduced photovoltaic properties of P3ATs with alkyl chain length greater or shorter than hexyl, the intrinsic carrier mobility of thin films of P3ATs is known to similarly vary with alkyl chain length.[20] Although not fully understood, the underlying mechanism for this large dependence of the photovoltaic and charge transport properties of P3ATs on alkyl chain length appears to include differences in solubility, self-assembly/crystallization and molecular packing of chains, dilution effect of the insulating alkyl chain on π-electron density, electronic energy levels, and the absorption spectra and coefficients. Of major current interest in the field is the

*Corresponding author. E-mail: jenekhe@u.washington.edu.

(1) Gunes, S.; Neugebauer, H.; Sariciftci, N. S. *Chem. Rev.* **2007**, *107*, 1324–1338.
(2) Thompson, B. C.; Frechet, J. M. J. *Angew. Chem., Int. Ed.* **2008**, *47*, 58–77.
(3) Blom, P. W. M.; Mihailetchi, V. D.; Koster, L. J. A.; Markov, D. E. *Adv. Mater.* **2007**, *19*, 1551–1566.
(4) Chen, L.-M.; Hong, Z.; Li, G.; Yang, Y. *Adv. Mater.* **2009**, *21*, 1434–1449.
(5) Dennler, G.; Scharber, M. C.; Brabec, C. J. *Adv. Mater.* **2009**, *21*, 1323–1338.
(6) Alam, M. M.; Jenekhe, S. A. *Chem. Mater.* **2004**, *16*, 4647–4656.
(7) Kim, Y.; Cook, S.; Tuladhar, S. M.; Choulis, S. A.; Nelson, J.; Durrant, J. R.; Bradley, D. D. C.; Giles, M.; McCulloch, I.; Ha, C.-S.; Ree, M. *Nat. Mater.* **2006**, *5*, 197–203.
(8) Yu, G.; Gao, J.; Hummelen, J. C.; Wudl, F.; Heeger, A. J. *Science* **1995**, *270*, 1789–1792.
(9) Halls, J. J. M.; Walsh, C. A.; Greenham, N. C.; Marseglia, E. A.; Friend, R. H.; Moratti, S. C.; Holmes, A. B. *Nature* **1995**, *376*, 498–500.
(10) Li, G.; Shrotriya, V.; Huang, J.; Yao, Y.; Moriarty, T.; Emery, K.; Yang, Y. *Nat. Mater.* **2005**, *4*, 864–868.
(11) Ma, W.; Yang, C.; Gang, X.; Lee, K.; Heeger, A. J. *Adv. Funct. Mater.* **2005**, *15*, 1617–1622.
(12) Nguyen, L. H.; Hoppe, H.; Erb, T.; Gunes, S.; Gobsch, G.; Sariciftci, N. S. *Adv. Funct. Mater.* **2007**, *17*, 1071–1078.
(13) Zhou, E.; Yamakawa, S.; Tajima, K.; Yang, C.; Hashimoto, K. *Chem. Mater.* **2009**, *21*, 4055–4061.
(14) Liang, Y.; Wu, Y.; Feng, D.; Tsai, S.-T.; Son, H.-J.; Li, G.; Yu, L. *J. Am. Chem. Soc.* **2009**, *131*, 56–57.
(15) Bull, T. A.; Pingree, L. S. C.; Jenekhe, S. A.; Ginger, D. S.; Luscombe, C. K. *ACS Nano* **2009**, *3*, 627–636.
(16) Wu, P.-T.; Bull, T.; Kim, F. S.; Luscombe, C. K.; Jenekhe, S. A. *Macromolecules* **2009**, *42*, 671–681.
(17) Blouin, N.; Michaud, A.; Gendron, D.; Wakim, S.; Blair, E.; Neagu-Plesu, R.; Belletete, M.; Durocher, G.; Tao, Y.; Leclerc, M. *J. Am. Chem. Soc.* **2008**, *130*, 732–742.
(18) Xin, H.; Kim, F. S.; Jenekhe, S. A. *J. Am. Chem. Soc.* **2008**, *130*, 5424–5425.
(19) Gadisa, A.; Oosterbaan, W. D.; Vandewal, K.; Bolsee, J.-C.; Bertho, S.; D'Haen, J.; Lutsen, L.; Vanderzande, D.; Manca, J. V. *Adv. Funct. Mater.* **2009**, *19*, 3300–3306.
(20) Babel, A.; Jenekhe, S. A. *Synth. Met.* **2005**, *148*, 169–173.

Published on Web 02/09/2010

development of new approaches that can improve the BHJ materials and associated solar cells.

In the search of novel materials for improving the performance of polymer photovoltaic devices, block copolymers have recently attracted interest because of their intrinsic ability to form nanoscale domains by self-assembly.[21−32] Block copolymers have been explored in the fabrication of solar cells along three directions. First, BHJ devices free of fullerene have been made from diblock copolymers that incorporate electronically active donor and acceptor blocks; this is exemplified by poly(4-vinyltriphenylamine)-*b*-poly(perylene bisimide acrylate) from which an efficiency of 0.07% PCE was achieved.[24,25] Another example along this line is the diblock copolymer poly(3-hexylthiophene-*b*-perylene diimide) from which a 0.49% PCE was observed.[26] Second, diblock copolymers have been used as compatibilizers to stabilize the nanoscale morphology of poly(3-hexylthiophene) (P3HT)/fullerene and P3HT/perylene diimide blends. The nanoscale morphology and overall performance of P3HT:$PC_{61}BM$ and P3HT:perylene diimide BHJ solar cells were improved by using a P3HT-*b*-poly(fullerene) diblock[27] and a P3HT-*b*-poly(perylene diimide) diblock,[28] respectively. Third, diblock copolymers have been used as templates to fabricate devices with a 3D-bicontinuous morphology.[29−31] This is exemplified by the use of poly(4-fluorostyrene)-*b*-poly(D, L-lactide) as a bicontinuous gyroid network template to fabricate titania-based dye-sensitized solar cells.[29,30]

In this paper, we report an alternative block copolymer strategy toward improvement of BHJ polymer solar cells. By using a crystalline−crystalline diblock copoly(3-alkylthiophene) as the donor component in fullerene-based BHJ polymer solar cells, we have found a strong dependence of device performance on block composition and observed a substantial enhancement of the photovoltaic properties compared to those of the parent homopolymers. BHJ solar cells fabricated from blends of diblock poly(3-butylthiophene)-*b*-poly(3-octylthiophene) with fullerene ($PC_{71}BM$) were found to have efficiency of up to 3.0% PCE, which represents factors of 1.6−9 improvements in the efficiencies of the homopolymer (P3BT:$PC_{71}BM$ and P3OT:$PC_{71}BM$) devices. Our results demonstrate that by virtue of the unique capability of block copolymers to integrate multiple or even conflicting functionalities (e.g., solubility, self-assembly, interlayer/intermolecular distances, etc.) into one polymeric material, they offer a promising approach to advanced materials for polymer solar cells.

Chart 1. Structures of the Diblock Copolythiophenes, P3BT-*b*-P3OT (denoted BOx), and $PC_{71}BM$

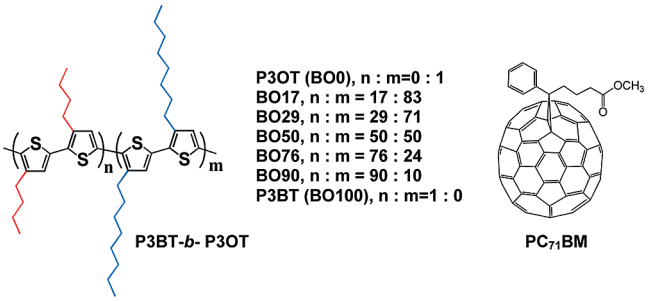

The molecular structures of the diblock copoly(3-alkylthiophene)s, poly(3-butylthiophene)-*b*-poly(3-octylthiophene) (P3BT-*b*-P3OT, denoted as BOx, where x is the mol % of the P3BT block), the two parent homopolymers (P3OT and P3BT), and [6,6]-phenyl C_{71}-butyric acid methyl ester ($PC_{71}BM$) are shown in Chart 1. The diblock copolymer P3BT-*b*-P3OT by design carries one block (P3BT) with short insulating butyl side groups and thus poor solubility, enhanced self-assembly, and efficient π-stacking of chains and the other block (P3OT) has good solubility, retarded self-assembly and π-stacking of chains, and long insulating octyl side groups. We seek to use the different side chains incorporated into the diblock P3BT-*b*-P3OT to balance and optimize the solubility, self-assembly, and π-stacking effects of the insulating side groups and thus the electronic and optoelectronic properties. Our studies included the optical and charge transport properties, fabrication and evaluation of BHJ solar cells, and investigation of the morphology of binary blends of $PC_{71}BM$ with each diblock copolymer BOx.

Experimental Section

Materials. Samples of P3BT (M_n = 107 900 g/mol, PDI = 3.61) and $PC_{71}BM$ (>99.0%) were obtained from American Dye Sources Inc. (Quebec, Canada). The as-received P3BT sample was subjected to Soxhlet extraction by hexane, dichloromethane, tetrahydrofuran (THF), and then chloroform. The THF-soluble fraction denoted P3BT-1 was collected and precipitated into methanol. The P3BT-1 sample had a M_n of 13 900 g/mol and a PDI of 1.07 as characterized by GPC. A sample of P3OT (M_n = 330 000 g/mol, PDI = 1.37) was synthesized using $Ni(dppe)Cl_2$ as catalyst, following the literature method.[33] A lower molecular weight sample of P3OT (denoted P3OT-1) was also synthesized by the literature method using $Ni(dppe)Cl_2$ as catalyst.[33] The resulting purple solid (P3OT-1) was purified by

(21) Eckert, J.-F.; Nicoud, J.-F.; Nierengarten, J.-F.; Liu, S.-G.; Echegoyen, L.; Barigelletti, F.; Armaroli, N.; Ouali, L.; Krasnikov, V.; Hadziioannou, G. *J. Am. Chem. Soc.* **2000**, *122*, 7467–7479.
(22) Jenekhe, S. A.; Chen, X. L. *Science* **1998**, *279*, 1903–1907.
(23) Chen, X. L.; Jenekhe, S. A. *Macromolecules* **1996**, *29*, 6189–6192.
(24) Lindner, S. M.; Huttner, S.; Chiche, A.; Thelakkat, M.; Krausch, G. *Angew. Chem., Int. Ed.* **2006**, *45*, 3364–3368.
(25) Sommer, M.; Huttner, S.; Wunder, S.; Thelakkat, M. *Adv. Mater.* **2008**, *20*, 2523–2527.
(26) Zhang, Q.; Cirpan, A.; Russell, T. P.; Emrick, T. *Macromolecules* **2009**, *42*, 1079–1082.
(27) Sivula, K.; Ball, Z. T.; Watanabe, N.; Frechet, J. M. J. *Adv. Mater.* **2006**, *18*, 206–210.
(28) Rajaram, S.; Armstrong, P. B.; Kim, B. J.; Frechet, J. M. J. *Chem. Mater.* **2009**, *21*, 1775–1777.
(29) Crossland, E. J. W.; Kamperman, M.; Nedelcu, M.; Ducati, C.; Wiesner, U.; Smilgies, D. M.; Toombes, G. E. S.; Hillmyer, M. A.; Ludwigs, S.; Steiner, U.; Snaith, H. J. *Nano Lett.* **2009**, *9*, 2807–2812.
(30) Crossland, E. J. W.; Nedelcu, M.; Ducati, C.; Ludwigs, S.; Hillmyer, M. A.; Steiner, U.; Snaith, H. J. *Nano Lett.* **2009**, *9*, 2813–2819.
(31) Botiz, I.; Darling, S. B. *Macromolecules* **2009**, *42*, 8211–8217.
(32) Wu, P.-T.; Ren, G.; Kim, F. S.; Li, C.; Mezzenga, R.; Jenekhe, S. A. *J. Polym. Sci., A: Polym. Chem.* **2010**, *48*, 614–626.
(33) Heeny, M.; Zhang, W.; Duffy, W.; McCulloch, I.; Koller, G. World Patent Application WO2007/059838, **2007**.

Soxhlet extraction using methanol, acetone, hexane, and finally dichloromethane. The P3OT-1 sample (dichloromethane-soluble fraction) precipitated into methanol and dried had a M_n of 21 600 g/mol with a PDI of 2.21 as characterized by GPC. The synthesis of some of the diblock P3BT-*b*-P3OT samples (BO50, BO76) by quasi-living polymerization was previously reported.[34] The synthesis of BO17, BO29, and BO90 was carried out using the same reagents and conditions.[34,35] In the diblock copolymer P3BT-*b*-P3OT, denoted BOx (x = 17, 29, 50, 76, and 90), the composition variable x is the percent mole fraction of P3BT segment in the diblock copolythiophene. BO17, BO29, and BO90 were similarly characterized by GPC (120 °C, eluent: 1,2,4-trichlorobenzene).[35] BO17: M_n = 17 400, PDI = 1.76. BO29: M_n = 33 800, PDI = 1.62. BO90: M_n = 15 800, PDI = 2.84. The series of BOx copolymers all have a comparable M_n in the range of 11 400−17 400,[34] corresponding to about 75−110 thiophene units in the main chains, except BO29, which has about a factor of 2 higher molecular weight.

Blend (1:1, wt:wt) solutions of BOx, P3OT, or P3BT with $PC_{71}BM$ were prepared by dissolving and stirring them together in N_2-degassed ortho-dichlorobenzene (ODCB, Aldrich) until complete dissolution. For P3OT, BO17, BO29, and BO50, 40 mg mL^{-1} blend solutions were prepared at room temperature; for BO76, BO90, and P3BT, 40, 30, and 30 mg mL^{-1} blend solutions were prepared at 80 °C. All the blend solutions were passed through a 0.45 μm filter except P3BT (1.0 μm filter).

Device Fabrication and Characterization. Solar cells used for photovoltaic and incident photon-to-current efficiency (IPCE) measurements were prepared on ITO-coated glass (10 Ω/□, Shanghai B. Tree Tech, China). The substrates were cleaned sequentially with acetone, deionized water and isopropyl alcohol in an ultrasonic bath. A 50 nm PEDOT:PSS (Baytron P VP AI 4083) layer was spin-coated on top of ITO and dried at 150 °C for 10 min under vacuum. Each blend was spin-coated on top of the PEDOT:PSS layer for 30 s in a glovebox to make the active polymer blend layer of 80−110 nm. The devices were treated under one of three conditions: dried at 60 °C in vacuum for 2 h (condition 1), or aged in a Petri dish for 5 min (condition 2) or 30 min (condition 3) followed by drying at (110 ± 10) °C on a hot plate for 5 min. The devices were loaded in a thermal evaporator (BOC Edwards, 306), where a cathode consisting of 1.0 nm LiF and 80 nm Al was deposited through a shadow mask under high vacuum (8×10^{-7} Torr) to produce 5 solar cells with an active area of 3.57 mm^2 each, per substrate. Space-charge limited current (SCLC) devices were fabricated in a similar way, except that Au electrode was deposited instead of LiF/Al, to facilitate hole-only injection and transport. The current density−voltage ($J-V$) curves of both solar cells and SCLC devices were measured using a HP4155A semiconductor parameter analyzer under laboratory ambient air condition.[36] AM1.5 illumination at 100 mW/cm^2 was provided by a filtered Xe lamp and calibrated by using an NREL-calibrated Si diode.[36] Incident photon-to-current efficiency (IPCE) measurement was done by using an Oriel xenon lamp (450 W) with an Oriel Cornerstone 130 1/8 m monochromator. The signal was measured with a calibrated standard silicon solar cell and KG5 filter which was calibrated at NREL using a SR830 DSP lock-in amplifier at a chopping frequency of 400 Hz. SCLC characteristics were measured on the devices processed under condition 2 in dark condition. The zero-field SCLC hole mobility was obtained by using nonlinear least-squares fitting of the $J-V$ data according to the Mott−Gurney equation (eq 1):

$$J = \frac{9}{8}\varepsilon\varepsilon_0\mu\frac{V^2}{L^3}\exp\left(\frac{0.89\beta}{\sqrt{L}}\sqrt{V}\right) \quad (1)$$

where J is the current density, V is the applied voltage, L is the active layer thickness, μ is the mobility, ε is the relative permittivity, ε_0 is the permittivity of free space, and β is the field-activation factor.[37]

Characterization of Morphology. X-ray diffraction (XRD) was performed on the actual solar cells, whose photovoltaic properties are reported, using a Bruker F8 Focus Powder X-ray Diffractometer with Cu K_α beam (40 kV, 40 mA; λ = 0.15418 nm). Atomic force microscopy (AFM) imaging was performed on the same solar cell devices by using a Dimension 3100 SPM (Veeco) instrument operating in tapping mode. Thin films of the active layers were obtained by scratching edges of the thin films, soaking with water, and peeling them off from the device substrates, and they were then supported on TEM grids (Electron Microscopy Sciences) for bright-field transmission electron microscopy (BF-TEM) imaging. An FEI Tecnai G^2 F20 TEM at 200 kV was employed, with a 0.031 mm^2 aperture for selected area electron diffraction (SAED). TEM images were acquired with a CCD camera and recorded with Gatan DigitalMicrograph software. SAED for $PC_{71}BM$ was obtained from a film drop-casted from ODCB solution. UV−vis absorption spectra were recorded with a Perkin-Elmer model Lambda 900 UV/vis/near-IR spectrophotometer on the blend films spin-coated on top of PEDOT/ITO substrates, following the same drying conditions as the solar cells.

Results and Discussion

The absorption spectra of the BOx:$PC_{71}BM$ blend thin films and those of P3BT:$PC_{71}BM$ and P3OT:$PC_{71}BM$ are shown in Figure 1. The line shape of the spectra, absorption maxima, and absorption coefficients of the diblock copolymer blends are seen to vary slightly with the block composition. P3OT and P3BT blend thin films have absorption maxima at 513 and 462 nm, respectively. The absorption spectrum of P3BT:$PC_{71}BM$ blend thin films is similar to that previously reported based for P3BT:PCBM blends,[12] but is significantly blue-shifted compared to that reported for self-assembled P3BT nanowires.[18] The blue shift and less structure in the spectrum of P3BT are likely a result of the high polydispersity (PDI = 3.61) of this sample and its poor assembly into highly crystalline domains within the P3BT:$PC_{71}BM$ blend. The absorption maxima of the BOx:$PC_{71}BM$ blends all fall between those of P3OT and P3BT. Enhanced absorption in the 550−650 nm region with vibronic

(34) Wu, P.-T.; Ren, G.; Li, C.; Mezzenga, R.; Jenekhe, S. A. *Macromolecules* **2009**, *42*, 2317–2320.

(35) Characterization details. **BO17**, purple solid; yield, 1.87 g, 75.6%. Regioregularity: 93.9%. ^{1}H NMR ($CDCl_3$), δ (ppm): 7.0 (1H), 2.82−2.60 (2H), 1.77−1.67 (2H), 1.52−1.31 (8.64H), 1.03 (0.51H), 0.88 (2.49H) . GPC: M_n = 17 400, PDI = 1.76. **BO29**, purple solid; yield, 1.29 g, 86.7%. Regioregularity: 95.5%. ^{1}H NMR ($CDCl_3$), δ (ppm): 7.0 (1H), 2.86−2.58 (2H), 1.71−1.67 (2H), 1.54−1.32 (7.68H), 1.00 (0.87H), 0.88 (2.13H) . GPC: M_n = 33 800, PDI = 1.62. **BO90**, purple solid; yield, 1 g, 59.2%. Regioregularity: 94.1%. ^{1}H NMR ($CDCl_3$), δ (ppm): 7.0 (1H), 2.86−2.59 (2H), 1.76−1.63 (2H), 1.52−1.31 (2.8H), 1.00 (2.7H), 0.88 (0.3H) . GPC: M_n = 15 800, PDI = 2.84.

(36) Xin, H.; Guo, X.; Kim, F. S.; Ren, G.; Watson, M. D.; Jenekhe, S. A. *J. Mater. Chem.* **2009**, *19*, 5303–5310.

(37) Murgatroyd, P. N. *J. Phys. D: Appl. Phys.* **1970**, *3*, 151–156.

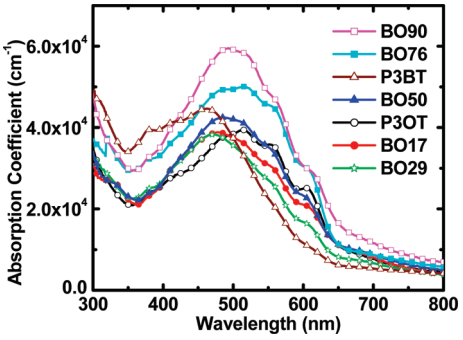

Figure 1. Absorption spectra of BOx:$PC_{71}BM$ (1:1, wt:wt) blend thin films dried at 60 °C in vacuum.

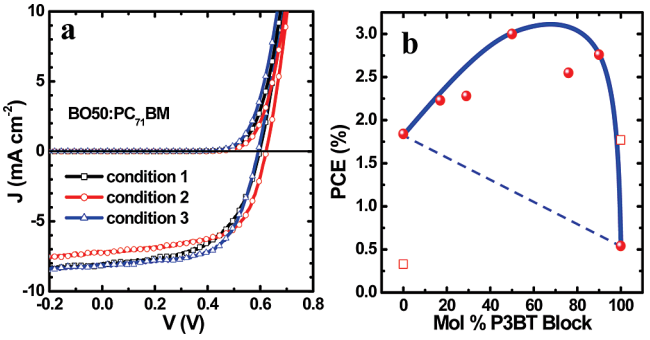

Figure 2. (a) Current density−voltage characteristics of BO50:$PC_{71}BM$ solar cells processed at different conditions: Condition 1, dried at 60 °C in vacuum; Condition 2, 5 min film aging in a Petri dish and 5 min thermal annealing at 110 °C; Condition 3, 30 min film aging in a Petri dish and 5 min thermal annealing at 110 °C. (b) Compositional dependence of the highest efficiency of solar cells with BOx active layers. The trend line is drawn as a guide to eye. The PCE of P3BT-1 and P3OT-1 devices are indicated by open square (□).

shoulders at 560 and 600 nm, indicative of improved interchain π-stacking and crystalline domains in some of the BOx phase are observed (Figure 1).[38] The peak absorption coefficients are in the range of 3.8×10^4 to 6.0×10^4 cm^{-1} for BOx:$PC_{71}BM$ blend thin films with $x = 50-90$ mol % P3BT, which are larger than the peak absorption coefficient of P3OT:$PC_{71}BM$ blend. The higher peak absorption coefficients of blend thin films of some of the diblock copolymers, compared to those of the homopolymers, in some spectra regions suggest enhanced harvesting of the solar spectrum in BHJ devices. The enhanced absorption coefficient in some of the diblock copolymers can be understood in terms of a higher degree of crystallinity in those samples.

The photovoltaic properties of BHJ solar cells using the diblock copolythiophenes as the donor component and $PC_{71}BM$ as the acceptor were investigated in comparison with those of the parent homopolymer (P3BT and P3OT) solar cells. The BHJ devices were of the basic structure ITO/PEDOT:PSS/active layer/LiF/Al, where the active layer is a BOx:$PC_{71}BM$ or a P3OT:$PC_{71}BM$ or a P3BT:$PC_{71}BM$ blend thin film. All the solar cells were characterized under AM1.5 solar irradiation at 1 sun (100 mW/cm^2) in ambient air. The current density (J) − voltage (V) curves for BO50:$PC_{71}BM$ blend thin film solar cells processed under three conditions are shown in Figure 2a. A slight improvement in the photocurrent and overall device efficiency was observed by going from vacuum drying of the blend thin films at 60 °C (condition 1) to film aging and thermal annealing (conditions 2 and 3). The photovoltaic parameters derived from Figure 2a and similar plots for BOx:$PC_{71}BM$ blend devices, including the short-circuit current density (J_{sc}), the open circuit voltage (V_{oc}), the fill factor (FF), and the maximum PCE for each polymer are summarized in Table 1. The observed open circuit voltage (0.56−0.65 V) in solar cells incorporating the series of block copolymers are comparable to those of the homopolymers, P3BT (0.54 V) and P3OT (0.66 V). However, there is a significant increase of both the photocurrent and fill factor of the block copolymer devices compared to those of either P3BT or P3OT. Indeed, these improvements in J_{sc} and FF translate to a large enhancement in the power conversion efficiency

Table 1. Summary of Charge Transport and Photovoltaic Properties of BO*x*:$PC_{71}BM$ Blend Thin Films[a]

BOx:$PC_{71}BM$ (1:1 wt:wt)	μ_h (cm^2 V^{-1} s^{-1})[b]	J_{sc} (mA cm^{-2})	V_{oc} (V)	FF	PCE (%)
P3OT	3.64×10^{-5}	5.81	0.66	0.48	1.84[b]
P3OT-1	2.31×10^{-8}	1.58	0.65	0.33	0.33[b]
BO17	1.53×10^{-5}	7.05	0.65	0.49	2.23[b]
BO29	2.38×10^{-4}	7.06	0.62	0.52	2.28[b]
BO50	2.50×10^{-4}	8.09	0.59	0.63	3.00[c]
BO76	8.04×10^{-5}	7.41	0.61	0.57	2.55[c]
BO90	2.76×10^{-4}	7.90	0.56	0.63	2.76[c]
P3BT	5.32×10^{-6}	2.24	0.54	0.45	0.54[c]
P3BT-1	1.15×10^{-7}	4.91	0.64	0.57	1.77[c]

[a] Spin-coated thin films of BOx:$PC_{71}BM$ (1:1, wt:wt) blends had thickness in the 80−110 nm range. [b] Processing condition 2. [c] Processing condition 3.

(PCE) of the BOx:$PC_{71}BM$ solar cells compared to the two homopolymers as shown in Figure 2b. The strong nonlinear dependence of solar cell efficiency (PCE) on block composition, showing enhancement relative to the homopolymers, suggest that the block composition could be an attractive variable for optimization of polymer solar cells. Among the block copolymer solar cells, BO50:$PC_{71}BM$ devices have the highest efficiency of 3.0% PCE and this represents factors of 6 and 1.6 enhancement relative to P3BT and P3OT homopolymers, respectively. The 1.84% PCE obtained for P3OT:$PC_{71}BM$ blends is the highest reported to date for P3OT-based solar cells; it is higher than 0.91% PCE previously reported for this polymer.[12] In the case of the P3BT homopolymer, our observed 0.54% PCE is higher than 0.27% PCE reported earlier by others[12] for similar BHJ (P3BT:PCBM) devices. BHJ devices made from P3OT-1 homopolymer, whose molecular weight is comparable to those of the block copolythiophenes, gave an efficiency of 0.33% PCE. This photovoltaic efficiency is significantly lower for the low molecular weight P3OT-1 compared to its higher molecular weight P3OT. In the case of P3BT-1, whose M_n value is also in the range of those of the BOx block copolymers, the photovoltaic efficiency of P3BT-1:$PC_{71}BM$ devices was 1.77% PCE which is significantly

(38) Erb, T.; Zhokhavets, U.; Hoppe, H.; Gobsch, G.; Al-Ibrahim, M.; Ambacher, O. *Thin Solid Films* **2006**, *511−512*, 483–485.

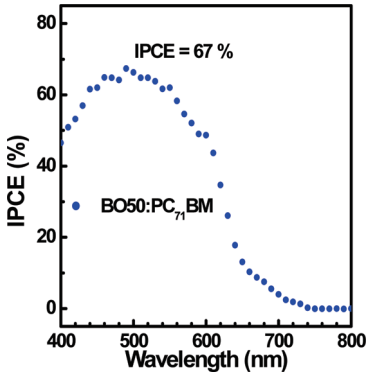

Figure 3. IPCE spectrum of a BO50:$PC_{71}BM$ (1:1) device prepared by condition 3 above.

higher than that of its higher molecular weight P3BT (0.54%) or literature values (0.27%).[12] Thus, the highest efficiency of 3.0% PCE seen in solar cells based on one of the BOx block copolythiophenes represents a factor of 1.6−9.1 enhancement compared to P3OT homopolymer and a factor of 1.7−5.6 enhancement compared to P3BT homopolymer. We note that the efficiency (3.0% PCE) observed for BO50:$PC_{71}BM$ is also in the range of those observed for P3HT/fullerene BHJ solar cells[1,2,10,11] and is comparable to those reported for the best P3BT nanowire-based devices.[18,19]

The photoaction or incident photon-to-current efficiency (IPCE) spectrum of the BO50:$PC_{71}BM$ blend solar cell is shown in Figure 3. The photoresponse of this BHJ diode turns on at about 730 nm and peaks at ~490 nm, giving a maximum IPCE of 67% electrons/photon. It is interesting that this IPCE value is very close to those reported for P3HT/fullerene BHJ solar cells.[39,40]

To better understand the photovoltaic properties of these diblock copolythiophenes compared with their parent homopolymers, we studied the surface and bulk morphologies of the blend thin films by atomic force microscopy (AFM) and transmission electron microscopy (TEM). The AFM phase images of BOx:$PC_{71}BM$ (x = 0, 50, 90 and 100) blend thin films are shown in Figure 4 a−d and those for BOx:$PC_{71}BM$ (x = 17, 29 and 76) blend thin films are given in Figure S1a−c in the Supporting Information. Nanoscale mixing between BOx and $PC_{71}BM$ is seen in the surface morphology of the blend thin films with x = 0 and 50−100, and small $PC_{71}BM$ domains are distributed among the polymer matrices. In the case of BO17:$PC_{71}BM$ and BO29:$PC_{71}BM$ blend thin films, macrophase separation was visually observed immediately after spin-coating. This phase separation is also evidenced by the distinct two phases identified in BO17:$PC_{71}BM$ blend thin film (see Figure S1a in the Supporting Information) and the two different surface morphologies seen in BO29:$PC_{71}BM$ (see Figure S1b in the Supporting Information). Bright-field TEM imaging of the BOx:$PC_{71}BM$ blend thin films under a slightly defocused condition provided good phase contrast between polymer and $PC_{71}BM$ domains, as exemplified by the micrographs shown in Figure 4e−h and Figure S1d−f in the Supporting Information. A network of fibrilar nanostructures observed in all the BOx:$PC_{71}BM$ blend thin films is characteristic of the polymer domains, whereas the $PC_{71}BM$ domains are distributed around the polymer networks. The width of these nanostructures is about 11−18 nm in all the BOx:$PC_{71}BM$ blend thin films, but the length of the nanowires varies, for example, 500−2500 nm in BO50:$PC_{71}BM$. These polymer nanostructures are reminiscent of those formed by solution-phase self-assembly of P3BT or BO50.[18,34,41] The interpenetrating, quasi-bicontinuous, polymer/fullerene network revealed by TEM imaging of BOx:$PC_{71}BM$ blend thin films clearly facilitates charge carrier photogeneration and transport.

Selected area electron diffraction (SAED) was performed on the same BOx:$PC_{71}BM$ blend thin films used for TEM imaging to obtain a measure of their crystallinity. The SAED pattern of pure $PC_{71}BM$ film acquired as a reference (see Figure S2 in the Supporting Information) showed two distinct Debye−Scherrer diffraction rings, corresponding to d-spacings of 0.49 and 0.33 nm.[42,43] The SAED patterns of the BOx:$PC_{71}BM$ blend thin films are shown in the insets of Figure 4e−h and Figure S1d−f in the Supporting Information. The diffraction peaks around q = 2.5−2.9 nm^{-1} in reciprocal space agree with the (020) reflections of P3AT crystals with random orientations, indicating that the $\pi-\pi$ stacking distances are within the range of 0.35−0.40 nm (see Figure S3 in the Supporting Information) and in good agreement with a previously reported value of 0.38 nm.[42,44] The peaks around q = 1.99−2.23 nm^{-1} are due to the diffraction of $PC_{71}BM$, with a d-spacing around 0.45−0.50 nm.[42,43] These SAED results mean that the block copolymers form crystalline domains in the blend thin films, and that the $PC_{71}BM$ aggregates observed in AFM and TEM are nanocrystallites. The formation of crystalline donor and acceptor phases in the blend thin films is important for charge transport.

The crystallinity and molecular packing of the BOx:$PC_{71}BM$ thin films were further confirmed by X-ray diffraction (XRD) conducted on the same solar cells as characterized in Figures 2 and 3 and the XRD spectra are shown in Figure 5. In P3OT:$PC_{71}BM$ and P3BT:$PC_{71}BM$ blends, interchain spacings (d_{100}) of 1.91 and 1.24 nm were observed, respectively. In the case of the BOx:$PC_{71}BM$ blends, they are expected to show two distinct crystalline domains with different d-spacings, because of the different interlayer distances of d_{P3OT} and d_{P3BT}.[34] However, except for BO50, in which two distinct reflections at 1.95 nm

(39) Li, G.; Yao, Y.; Yang, H.; Shrotriya, V.; Yang, G.; Yang, Y. *Adv. Funct. Mater.* **2007**, *17*, 1636–1644.
(40) Padinger, F.; Rittberger, R. S.; Sariciftci, N. S. *Adv. Funct. Mater.* **2003**, *13*, 85–88.
(41) Xin, H.; Ren, G.; Kim, F. S.; Jenekhe, S. A. *Chem. Mater.* **2008**, *20*, 6199–6207.
(42) van Bavel, S. S.; Sourty, E.; de With, G.; Loos, J. *Nano Lett.* **2009**, *9*, 507–513.
(43) Yang, X.; van Duren, J. K. J.; Rispens, M. T.; Hummelen, J. C.; Janssen, R. A. J.; Michels, M. A. J.; Loos, J. *Adv. Mater.* **2004**, *16*, 802–806.
(44) Ihn, K. J.; Moulton, J.; Smith, P. *J. Polym. Sci., Part B* **1993**, *31*, 735–742.

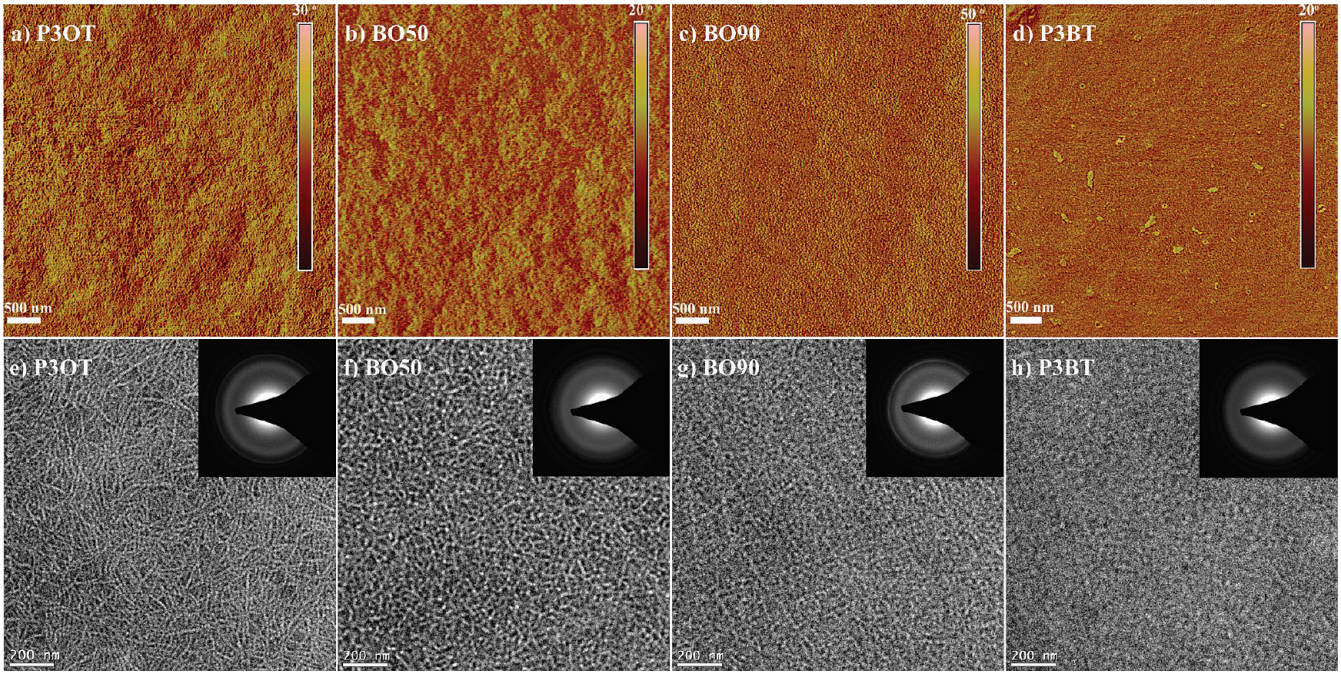

Figure 4. (a−d) AFM phase images and (e−h) TEM images (inset: SAED pattern) of BOx:$PC_{71}BM$ blend thin films (x = 0, 50, 90, 100). The thin films were prepared by 5 min film aging in a Petri dish and 5 min thermal annealing at 110 °C (condition 2).

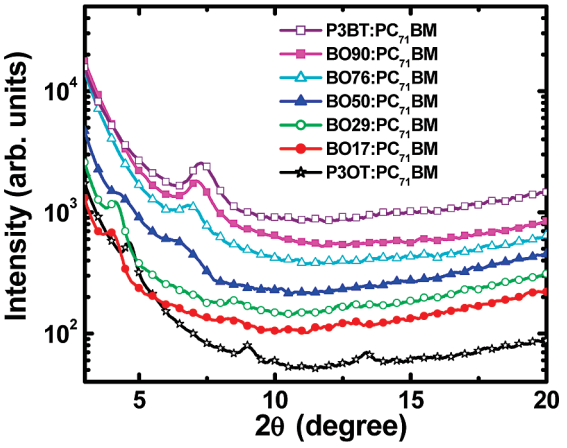

Figure 5. XRD spectra of BOx:$PC_{71}BM$ blend films obtained directly from the solar cell devices.

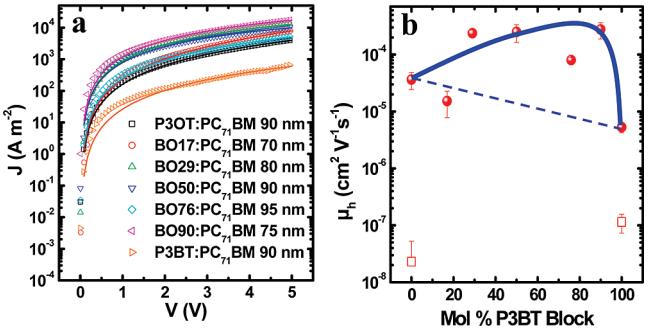

Figure 6. (a) Dark current density−voltage (J−V) characteristics of ITO/PEDOT:PSS/BOx:$PC_{71}BM$/Au for SCLC measurement of mobility and model fitting of the data. (b) Block compositional dependence of SCLC hole mobility of BOx:$PC_{71}BM$ blend thin films. The trend line is drawn as a guide to eye. The SCLC hole mobility of P3BT-1:$PC_{71}BM$ and P3OT-1:$PC_{71}BM$ blends are indicated by open square (□).

(d_{P3OT}) and 1.46 nm (d_{P3BT}) with nearly equal relative intensities were detected, only the dominant reflection was revealed in the other BOx blends. This observation can be understood considering the small film thickness (80−110 nm) and the varying copolymer composition. The d_{P3OT} values seen in BO17 and BO29 are 2.22 and 2.14 nm, whereas the d_{P3BT} values observed in BO76 and BO90 are 1.43 and 1.24 nm, respectively. Compared with P3OT, the larger d_{P3OT} values in BO17 and BO29 indicate that molecular packing of these two block copolymers is significantly modified by $PC_{71}BM$. All the other BOx show decreased interlayer distances in the P3OT domains and increased interlayer distances in the P3BT domains.[34] The average interlayer distance in BO50 is 1.71 nm, which is close to that of P3HT (1.65 nm).[12] This interlayer distance seems to yield the best photovoltaic properties of solar cells based on P3AT:fullerene binary blends, because it maintains a reasonable polymer/fullerene phase separation, while maximizing the volume density of light absorbing backbone that leads to a higher photocurrent.

To gain insights into charge transport in the block copolythiophene solar cells, we used the space charge limited current (SCLC) method to evaluate the mobility of holes using ITO/PEDOT:PSS/active layer/Au as the hole-only devices. Figure 6a shows the dark-current density (J)−voltage (V) characteristics of these BOx:$PC_{71}BM$ devices; these data were analyzed using the Mott−Gurney equation[37] and prior procedures.[41] The zero-field mobility (μ_h) of holes in BOx:$PC_{71}BM$ blends are summarized in Table 1. The hole mobility varies from 2.3×10^{-8} cm^2 V^{-1} s^{-1} in P3OT-1:$PC_{71}BM$ to 2.8×10^{-4} cm^2 V^{-1} s^{-1} in BO90:$PC_{71}BM$ (Table 1). The block compositional dependence of the SCLC hole mobility, $\mu(x)$, in BOx:$PC_{71}BM$ blend films is shown in Figure 6b.

We note that the hole mobility of both homopolymers and homopolymer/PCBM blends varies significantly with molecular weight. Compared with the P3OT and P3BT homopolymers, almost all of the diblock copolymers show enhanced hole transport (Figure 6). The μ_h values for BO29, BO50, and BO90 blend thin films are orders of magnitude higher than those of P3OT and P3BT, respectively. The enhanced charge transport in the block copolythiophene/fullerene blends can be understood in terms of the facile self-assembly of highly crystalline nanostructures in the spin-coated thin films (Figure 4) as observed by TEM/SAED and XRD.

The SCLC mobility of holes in pure BOx thin films was also measured for comparison with the BOx:$PC_{71}BM$ BHJ films. Figure S4a shows the $J-V$ characteristics of the ITO/PEDOT:PSS/BOx/Au devices and the SCLC hole mobility is plotted as a function of block composition (Mol % P3BT) in Figure S4b in the Supporting Information. The block composition dependence of hole mobility observed in BOx thin films is very similar to that seen in the BHJ BOx:$PC_{71}BM$ blends. Most of the block copolymers have SCLC hole mobilities that are comparable for both blend thin films and the pure BOx thin films. The lower hole mobility in BO17:$PC_{71}BM$ thin films, compared to the other BOx diblock copolymers and pure BO17 thin films, is an anomaly because of macrophase separation between BO17 and $PC_{71}BM$. Overall, the SCLC hole mobility of the block copolymers (BO29, BO50 and BO90) is comparable with that reported for annealed P3HT:$PC_{61}BM$ (1:1) blend films exhibiting high photovoltaic efficiency (3% PCE), which is 2×10^{-4} cm^2 V^{-1} s^{-1}.[45] The observed dependence of carrier mobility on block composition (Figure 6b) is remarkably similar to the previously discussed dependence of the power conversion efficiency of solar cells on block copolymer composition. This suggests that enhanced charge transport is a major contribution to the observed improvement in the efficiency of BHJ solar cells based on the diblock copolythiophenes.

(45) Mihailetchi, V. D.; Xie, H.; de Boer, B.; Koster, L. J. A.; Blom, P. W. M. *Adv. Funct. Mater.* **2006**, *16*, 699–708.

Conclusions

We have investigated the photovoltaic and charge transport properties and morphology of bulk heterojunction solar cells based on a series of diblock copoly(3-alkylthiophene)s. Our results have shown that crystalline block copoly(3-alkylthiophene)s have substantially enhanced photovoltaic properties compared to the parent homopolymers. AFM and TEM imaging in conjunction with XRD/SAED showed that the P3BT-*b*-P3OT/$PC_{71}BM$ blends had an interpenetrating morphology with crystalline polymer domains (11−18 nm). Studies of BHJ solar cells based on poly(3-butylthiophene)-*b*-poly(3-octylthiophene) and fullerene derivative ($PC_{71}BM$) showed that the power conversion efficiency strongly depends on the block composition, reaching a maximum value of 3.0% PCE at 50 mol % P3BT. This efficiency is about a factor of 1.6−9 times higher than the corresponding homopolymer devices made under similar conditions. The observed enhancement of carrier mobility of holes in the BHJ devices largely accounts for the large improvement in photovoltaic efficiency and its dependence on block copolythiophene composition. These results demonstrate that block conjugated copolymers represent a promising strategy in the design and optimization of polymer semiconductors for low-cost solar energy conversion devices.

Acknowledgment. Our report is based on research (polymer and organic/inorganic hybrid solar cells) supported by the U.S. DOE, Basic Energy Sciences, Division of Materials Science, under Award No. DE-FG02-07ER46467. S.A.J. also acknowledges the NSF (DMR-0805259 and DMR-0120967) for support of the synthesis of polymer semiconductors. G.R. received a University of Washington Initiatives Fund (UIF) fellowship from the UW Center for Nanotechnology. Part of this work was conducted at the University of Washington NanoTech User Facility, a member of the NSF National Nanotechnology Infrastructure Network (NNIN). We thank Dr. Hao Xin for useful discussions and Steven Hau for IPCE measurement.

Supporting Information Available: Additional AFM and TEM images, SAED of PCBM and block copolymer blends, and SCLC data of polymer thin films (PDF). This material is available free of charge via the Internet at http://pubs.acs.org.